Further improvements in the structural analysis of DEMO Divertor Cassette body and design assessment according to RCC-MRx

Paolo Frosi[a], Pietro Alessandro Di Maio[b], Domenico Marzullo[c], Giuseppe Mazzone[a], Jeong-Ha You[d],

[a] *Department of Fusion and Technology for Nuclear Safety and Security, ENEA C. R. Frascati, via E. Fermi 45, 00044 Frascati (Roma), Italy*
[b] *University of Palermo, Viale delle Scienze, Edificio 6, 90128 Palermo, Italy*
[c] *CREATE Consortium/University of Naples Federico II, Department of Industrial Engineering (DII), Piazzale Tecchio 80 – 80125 Napoli, Italy*
[d] *Max Planck Institute for Plasma Physics, Boltzmann Str. 2, 85748 Garching, Germany*

This paper presents the enhancements related to the structural analyses of DEMO Divertor in the framework of the EUROfusion Power Plant Physics & Technology (PPPT) program. This activity started two years ago and its preliminary results were published in previous papers. It has been divided in some areas defined by the similarity of the matters they contain: the structural analysis, of utmost importance, has been preceded by a preliminary phase, like the geometry definition or the thermal and the electric-magnetic analysis for loads evaluation; then the structural analysis has been finally confirmed with further evaluations related to excessive deformation or plastic instability. This paper discusses the improvements adopted either in the preliminary analysis or in the main structural analysis. Specifically it highlights the introduction of the thermal and electro-magnetic loads application in terms of a detailed spatial distribution that is now available. More the supports have been introduced in the model and their structural behavior has been investigated considering their interaction with the cassette. The structural assessment, according to the Design and Construction Rules for Mechanical Components of Nuclear Installation (RCC-MRx), has been performed either for the cassette or for the attachments: for the former it is positive while for the latter case serious limitations have been found.

Keywords: FEM, DEMO, Divertor, structural analysis, thermal analysis, RCC-MRx

1. Introduction

This paper summaries the last enhancements obtained in the structural design of DEMO Divertor. This activity began two years ago with provisional outcomes of the structural analysis that, in turn, was using the preparatory analysis results obtained with some approximations. This work can be inserted in the nuclear fusion frame depicted in [1-3] and a summary of the previous study can be found in [4-6]. The whole design activity has been improved either in the preparatory studies (e.g. neutron analysis, geometric dimensioning, thermal analysis) or in the proper stress-strain evaluation. These improvements have allowed to overcome the simplified hypothesis of loads uniform distribution. The simulation of geometry attachments allows to understand their effects on the Cassette and to discover their problematic stress level. Every kind of load has been analyzed separately: so some qualitative deductions can be done by comparing the results obtained in each case (with the awareness that the component finds itself in a plastic state, so they can be summed very carefully). More, as previously done, a simplified but meaningful assessment according to RCC-MRx code has been executed.

2. Preparatory analysis

2.1 Geometry

This step relates to the gathering of all input data needed to perform the required structural analysis.

The new geometry of the Divertor Cassette has been the first supplying: its development has been described adequately in [7]. A complete image of the new geometry is reported in fig. 1.

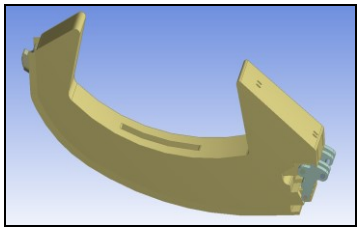

Fig. 1: 2016 CAD model of the Cassette Divertor

Neglecting all details that have been explained in [7], in comparison with the previous geometry [8], it must be highlighted the change of poloidal and toroidal internal ribs thickness from 30 to 20 mm, while the external cassette plates remain 30 mm thick.

2.2 Finite element model and materials

The Eurofer is the Cassette reference material: the Young modulus (E), the Poisson ratio (ν), the minimum yield strength at 0.2% ($R_{p0.2(min)}$), the minimum tensile strength ($R_{m(min)}$) and the maximum allowable stress (S_m) are reported in tab.1 as a function of temperature.

Tab. 1. Eurofer structural material properties

Temp (°C)	E (GPa)	ν	$R_{p0.2(min)}$ (MPa)	$R_{m(min)}$ (MPa)	S_m (MPa)
20	217	0.3	516	637	212
100	213	0.3	480	595	212
200	207	0.3	457	555	206
300	202	0.3	442	517	192
400	196	0.3	416	468	173

Corresponding author's email: paolo.frosi@enea.it

The specific heat capacity (C_p), the mass density (ρ), the thermal conductivity (λ), and the (secant) coefficient of thermal expansion (α) are reported in tab.2.

Tab. 2. Eurofer thermal material properties.

Temp (°C)	C_p (J/kgK)	ρ (kg/m^3)	λ (W/mK)	α (10^{-6}/K)
20	442	7760	28.34	10.3
100	495	7740	29.2	10.7
200	538	7713	30.67	11.2
300	574	7685	30.2	11.6
400	623	7655	29.33	11.9

The elastic-plastic material simulation has been the multilinear kinematic hardening model with constitutive parameters taken from [14]. The whole model has 196084 nodes and 105142 elements. The employed software has been Ansys release 18.2 [9].

The Divertor is fixed on the vacuum vessel through two different attachments that look like the ITER ones: the inboard one is called Nose and it is a sort of wedge that gives the right position to the Divertor inside the vessel, the second one is the knuckle with its pins that fixes statically the Divertor. They are plotted in fig. 2.

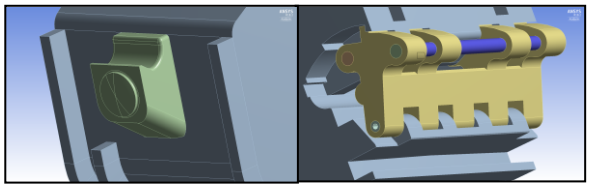

Fig. 2: view of attachments: Nose (left) and knuckle (right)

In all simulations the surface nodes of the Nose and of the external knuckle pin (that one attached to the vessel) have been constrained reproducing the cassette fixation upon the vessel. These attachments have a relevant role in the stress distribution as stated in the following.

2.3 Thermal loads input

The nuclear heating are the main set of data needed either for thermal or structural analysis. It has been evaluated with a detailed subdivision of the Divertor volume: the thermal power has been listed for each cell the Cassette has been divided in, as reported in [10].

This set of data has been adopted for the coupled–field thermal-fluid dynamic analysis reported in [11-12]. Unlike from the previous works [4-5], the thermal power has been applied exactly the same: so the temperature gradients have been simulated in a more realistic manner (and more adequate for the structural analysis purposes): in fig. 3 there is the obtained temperature contour plot.

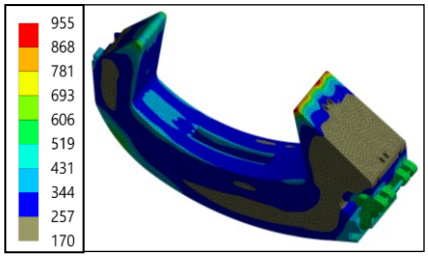

Fig. 3: temperature (°C) contour plot

The region at the top of the outer vertical targets that exhibits high temperatures can be neglected for a global structural analysis and it can be overcome with a more suitable geometric choice as stated in [8].

2.4 Magnetic load input

The same concept must be repeated for the electric-magnetic forces whose detailed distribution for the whole DEMO tokamak has been evaluated with another study [13]. Neglecting all details, the total forces acting on the Cassette Divertor have been reported in fig. 4 during the time interval across the disruption event (in this case downward major disruption) with clear symbolism of the directions they relate to. The radial direction is considered positive in the outward way, the vertical one is positive upward and the positive toroidal direction follows the cartesian reference right-hand rule.

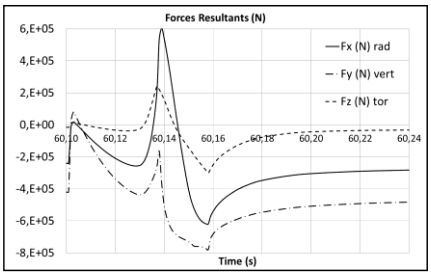

Fig. 4: EM Forces resultants on Divertor

3. Loads acting separately

These sets of input data allow to study the state of stress caused independently from one another.

3.1 Thermal loads

As obtained previously [4-5], the thermal loads play a relevant role: indeed in the fig. 5 there are the Nose (left), the cassette (center) and the knuckle pins (right) equivalent stresses: it can be seen that the stress level either of the Nose or the knuckle pins is relevant (350 - 500 MPa).

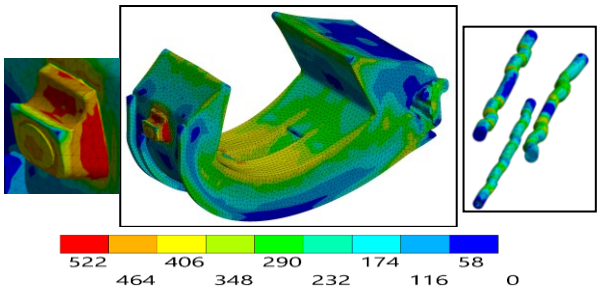

Fig. 5: Equivalent stresses (MPa) due to thermal loads

The highest stresses are on the Nose and this fact suggests to enlarge this attachment to spread the reaction forces over a wider region; the cassette region near the Nose suffers some plastic strain (≈ 2%) while in the knuckle region the plastic strain are about 10%: this fact will be more emphasized in the following cases and it is due to the overall deformation of the Cassette.

This high level of stress near the attachments can be predicted because now the thermal loads haven't been applied uniformly; indeed the material near the Dome region is hotter than that one in the bottom side and its greater lengthening can only result in an increase of curvature because the position of the attachments doesn't allow to the colder lower region to straighten as much as the upper central region. This finding is different from

what stated previously. In fig. 6 the radial displacements (superimposed to undistorted geometry) have been reported: it can be seen in the outer region a "butterfly distribution" as a proof of the curvature increase (the inner zone is practically fixed due to the Nose great stiffness).

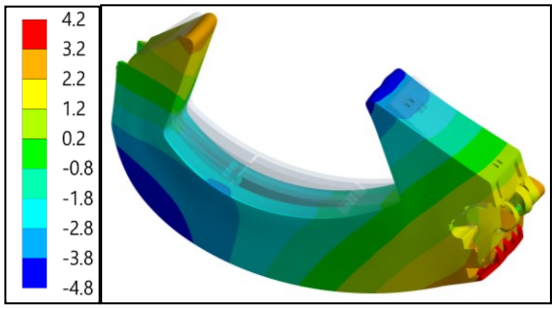

Fig. 6: radial displacements (mm) due to thermal loads

In the vertical displacement contour plot (not reported) the central zone that goes downward while the outer zone goes upwards can be observed as a coherent result with what stated previously.

3.2 Electric magnetic loads

For what concern the electro-magnetic loads, according to the fig. 4, two analysis have been done: one relative to the positive maximum (t=60.139 s) and one to the negative maximum (t=60.158 s). The import of the forces into the structural model considers surely the spatial distribution of the magnetic force density, but there is a great difference on mesh density (one related to the whole tokamak and one related only to a component), so the resultants in each direction (radial, vertical and toroidal) aren't preserved exactly during importation. The case more interesting (that is with the higher equivalent stresses) is the one at t=60.139 s (positive maximum): its equivalent stresses are reported in fig. 7 either for the cassette (left) or for the knuckle (right). In this case the high stresses occur in the knuckle housings and its pins (530 MPa): they are also subjected to a certain level of plastic stain (1%) while the cassette and the Nose are without plastic strain.

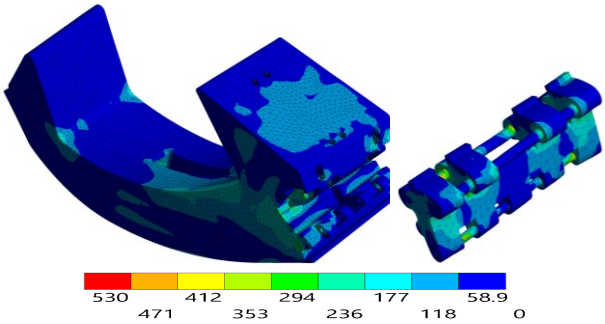

Fig. 7: equivalent stresses (MPa) due to magnetic forces

3.3 Pressure loads

The cooling water pressure has been the last load case studied. The last adopted values for the water are [11]: 3.5 MPa and 180°C for the inlet pressure and temperature respectively. In the fig. 8 there is the equivalent stress contour plot related to this case: now in the supports and in the cassette there aren't any plastic strain. The state of stress is globally low even though it's a little higher than that found previously due to the decreased thickness of the internal ribs.

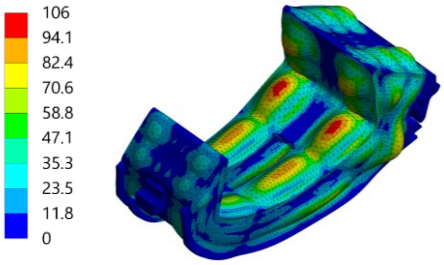

Fig. 8: equivalent stresses (MPa) due to applied pressure

4. Loads acting together

All the cases examined above are useful to understand the complete behavior of the Cassette when they acting together. Three cases have been analyzed:

4.1 Electric-magnetic and thermal loads

This case shows again that the thermal loads play a greater role than the EM forces: indeed the whole behavior of the cassette resembles far better the thermal loads case than the EM forces one. In the fig. 9 there is the related equivalent stress contour plot for the cassette (center), for the Nose (left) and for the Knuckle (right).

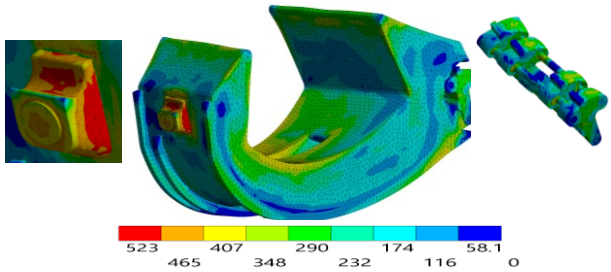

Fig. 9: equivalent stresses (MPa) due to thermal and EM loads

The highest stresses occur once again on the Nose and in the cassette region near the Nose. The former behaves like described in §3.1, the latter is subjected to high stresses because it is affected by the aforementioned increase of curvature (its upper part is stretched and its lower part is compressed) and this local field of displacement isn't accomplished by the Nose that is been fixed; more also the knuckle and its pins exhibits Von-Mises stresses still high. Indeed when only the thermal loads act, the radial reactions are equal and opposite (inboard reaction is directed outward and outboard reaction is directed inward), just like the vertical reactions that are directed downward (for the Nose) and upward (for the Knuckle); when the EM forces are superimposed it results a decrease of the inboard reaction absolute values (given by the EM radial and vertical forces resultants): the high equivalent stresses on the Nose can be explained with the fact that the reaction forces due to thermal loads (about 6 MN) are one order of magnitude greater than that due to EM forces (570 kN) and the latter can't influence so much the stress state in that region while in the knuckle pins the outboard reaction values remain the same. This fact reveals that the vessel compliance to the cassette deformation has a relevant impact on the resulting cassette and support structure stress level and it can be used as a way to limit

the cassette radial action on the vacuum vessel. Another coherent result is due to the cassette radial displacements contour plot (not reported) that is qualitative similar to that reported in fig. 6 when thermal loads act alone. More the knuckle pins exhibit high plastic strain that confirms the necessity to review their geometry.

4.2 Pressure and thermal loads

This case, regarding the pressure and thermal loads, can be put in the same frame of the previous ones. In fig. 10 the equivalent stress contour plot is reported either for the cassette (similar to fig. 5) or for the knuckle pins; also the Cassette radial displacement in this case is similar to what obtained in fig. 6 and it isn't reported.

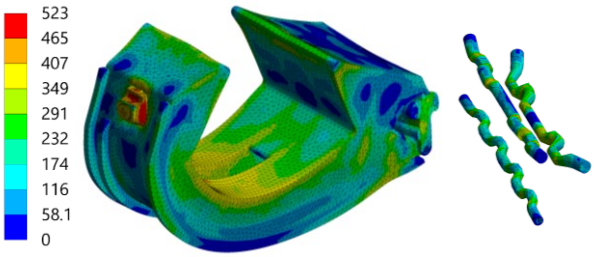

Fig. 10: equivalent stresses (MPa) due to thermal and pressure loads

As reported in the fig. 10 (right) the knuckle pins suffer again high stress (till to 400 MPa) and high plastic strain (till to 11% for the internal pin near the cassette); the knuckle stresses are lower than pins ones but relevant in any case (till to 350 MPa). Also here the cassette region near the Nose (affected by the bending action described in §4.1) exhibits a low plastic strain (≈1%).

4.3 Pressure, electric-magnetic and thermal loads.

The last case doesn't add any further information to what already stated because the pressure loads influence a little the global behavior of the Cassette. In fig. 11 there is the equivalent stress related to this case.

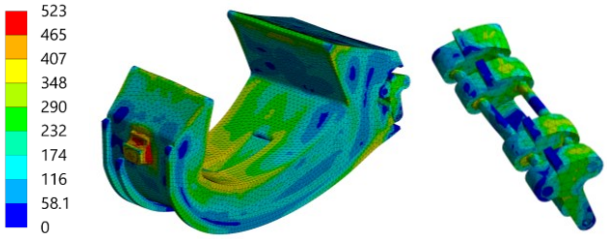

Fig. 11: equivalent stresses (MPa) caused by all loads

This case is a further repetition of the previous ones: the pressure and electric-magnetic loads essentially don't add any other contribution to the thermal loads effects: the Nose suffers the same stress level (with a plastic strain of about 2%), the cassette isn't affected by plastic strain except in the region near the Nose and in the housing of the knuckle pins (less than 1%); an high level of plastic strain is found in the knuckle housings (≈18%) and in the knuckle pins (>>20%): disregarding the mesh coarseness, these components must be fully revised.

The knuckle kinematic behavior is another proof of what stated previously: the knuckle follows the radial displacements "butterfly distribution" described in §2: the outer part of the Cassette due to the prevented radial lengthening tends to rotate (curvature increase in the Cassette central zone) and the knuckle follows this kind of deformation showing a radial displacement of the bottom hinge going outward.

5. RCC-MRx simplified assessment

A simplified evaluation according the RCC-MRx code (level A criteria) [13] has been performed. This verification is only illustrative because fatigue and buckling were not analyzed and, in line with the adopted hypothesis, it deals with the prevention from excessive deformation and ratcheting: nevertheless it shows how much the operative loads result far from the limit values. The aforementioned French nuclear code typically deals with the primary stresses (membrane P_m and bending P_b) and with the line supporting segments. The primary stresses are a linearization of the stresses (along the properly defined line supporting segments) that equilibrate directly the applied loads. This verification has been performed for the cassette and for the knuckle pins. The line supporting segments positions have been reported in fig. 12-13. The assessment has been performed only for un-irradiated conditions for the same reasons reported in [4-5].

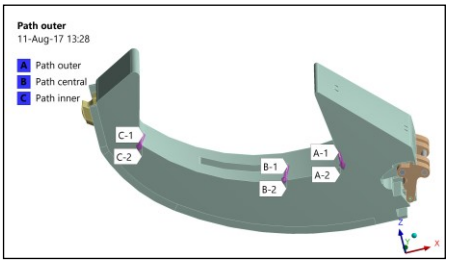

Fig. 12: line supporting segment on Cassette

This set of analysis has been executed adopting a linear elastic material properties. The first step is made to prevent type P damages (RCC-MRx Level A criteria): that is to verify that primary stresses due to mechanical loads (water pressure) at their operation temperature are below the admissible stresses at the same temperature.

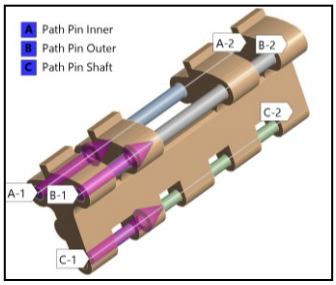

Fig. 13: line supporting segment on knuckle pins

Denoting with θ_m the mean temperature along the path and with S_m is the maximum allowable stress (temperature dependent values that are reported inside the code), the classical two relations for the three paths have been verified:

$$\overline{P}_m \le S_m(\vartheta_m) \tag{1}$$

$$\overline{P_m + P_b} \le 1.5 \cdot S_m(\theta_m) \tag{2}$$

where P_m is the general primary membrane stress intensity, P_m+P_b is primary membrane plus bending stress intensity: in table 3 there is the result of this step. The values related to the knuckle pins aren't been reported for their values far greater than allowable ones.

Tab. 3: verification against type P damages (values in MPa).

	P_m (MPa)	$S_m(\theta_m)$ (MPa)
Path outer (θ_m=249°C)	13.3	199
Path central (θ_m=283°C)	5.5	194
Path Inner (θ_m=326°C)	5.8	187
Path Inner Pin (ϑ_m=480°C)	*>>S_m*	*151.4*
Path Outer Pin (ϑ_m=523°C)	*>>S_m*	*136.1*
Path Lower Pin (ϑ_m=553°C)	*>>S_m*	*124.6*
	P_m+P_b (MPa)	1.5*S_m (MPa)
Path outer (θ_m=249°C)	19.5	299
Path central (θ_m=283°C)	13.2	292
Path Inner (θ_m=326°C)	7.3	281
Path Inner Pin (ϑ_m=480°C)	*>>1.5·S_m*	*227.2*
Path Outer Pin (ϑ_m=523°C)	*>>1.5·S_m*	*204.1*
Path Lower Pin (ϑ_m=553°C)	*>>1.5·S_m*	*186.9*

The second step is related to the stress range evaluation ($3S_m$ rule) that is the state of stress due to the full action of nuclear heating minus the state of stress due to stand-by condition (the component at the same temperature of bulk water) always written as ΔQ. This fact can be summarized by the relation:

$$Max\left(\overline{P_l + P_b}\right) + \overline{\Delta Q} \le 3 \cdot S_m \qquad (3)$$

The first term of this relation is the same of the previous analysis. With the same symbolism used in (3) and with the same θ_m values, in the tab. 4 the essential results have been reported. Also here the knuckle pins stress values clearly fail the $3S_m$ assessment (plastic strain higher than 10%) and they aren't been reported.

Tab. 4: verification against type S damages (values in MPa).

	(P_m P_b)+ΔQ (MPa)	3*$S_m(T_m)$ (MPa)
Path outer	157	597
Path central	186	583
Path inner	514	562

It can be written that, according the RCC-MRx simplified assessment, the three paths laying inside the Cassette show that the component is safe, while the other three paths laying along the knuckle pins (reported in tab. 3 in *italic*) show a huge level of stress (impossible in a plastic regime) that shows the need to improve the knuckle design.

6. Considerations about results

It has been found in every case that the stress level is dominated by thermal loads; the addition of pressure and electric-magnetic loads doesn't change so much the cassette and the supports stress level. The Nose withstands high radial stresses and determines a bending action in the nearby region due to its fixed position; the knuckle and its pins can't withstand the overall radial expansion: indeed the pins exhibit high plastic strains and their housings either on the cassette or on the knuckle are deformed over yield limit; it must be born in mind that the supports haven't been designed to allow thermal expansion and the vessel temperature hasn't been included in the analysis and this facts greatly affects the supports stress level.

Two summary tables report the highest equivalent stresses (tab. 5) and highest equivalent plastic strain (tab. 6) for the analyzed components to have a concise vision of the effects produced by all type of loads (th=thermal; em=electric-magnetic; pr=pressure).

Tab. 5: maximum equivalent stress for each component (MPa).

	cassette	knuckle	pins	Nose
th	522	352	401	522
em	407	414	530	112
pr	106	16	25	7
em+th	519	553	400	523
pr+th	523	352	402	522
pr+th+em	518	353	400	523

Tab. 6: highest equivalent plastic strain for each component.

(m/m)	cassette	knuckle	pins	Nose
th	2.2	16	11	2.2
em	0.1	0	1	0
pr	0	0	0	0
em+th	2.2	18	32	2.2
pr+th	2.4	16	11	2.2
pr+th+em	2.3	18	34	2.2

It can be stated that even though the cassette has an high level of stresses (that always happened in small regions and within very few elements), the corresponding plastic strain is always little and now it can be accepted considering all simplifications introduced in the model; instead the knuckle and its pins exhibit an high level of stress and a very high (impossible) plastic strain that brings to reject their geometry in the actual definition.

7. Advice for future work

The supports role is relevant: some generic improvements brought about their geometry and function can enhance the cassette operative conditions; a device (installed on vacuum vessel) that allows Nose very small rotations about a toroidal axis would be useful: it would accomplish the rotation of the cassette inboard region thus reducing the aforementioned bending action in the region near the Nose. For what concerns the outboard support, a device that applies a preload between the cassette and the knuckle either in stand-by condition or at full loading would keep it in the correct position; a unique increase of the pins diameter isn't recommended because it would decrease their state of stress but it wouldn't accomplish the radial displacements "butterfly distribution": so the pins arrangement should be revised in order to follow the radial lengthening described in §3.1 (e.g. overturning the knuckle with upper side placed in the bottom and vice versa). In the future analysis it must be considered also the role of the vacuum vessel temperature to influence the relative displacements of the vessel fixation point and the following knuckle kinematic behavior.

8. Conclusions

A complete and detailed elastic-plastic analysis has been performed for the Demo Divertor Cassette. The

uniform application of thermal and magnetic loads has been overcome: the actual precise distribution has allowed to know better the kinematic behavior of the Divertor Cassette. It is found once again that the thermal loads exhibit the greater influence on the component (in this case the support reactions are 10 times higher than that caused by electric-magnetic loads); so it tends to lengthen itself and to increase its curvature (as stated above). This creates a high state of stress for the Nose and high plastic strains for the Knuckle, its pins and the pin housing on the Cassette. The outboard region of the Cassette shows a sort of rotation with radial outward and vertical upward displacements. This fact suggests to review the knuckle geometry and the pins positions in order to accomplish such field of displacements. The RCC-MRx structural assessment, has been performed either for the cassette or for the attachments: for the former it is positive while for the latter case serious limitations have been found.

Acknowledgments

This work has been carried out within the framework of the EUROfusion Consortium and has received funding from the Euratom research programme 2014-2018. The views and opinions expressed herein do not necessarily reflect those of the European Commission.

The computing resources and the related technical support used for this work have been provided by CRESCO/ENEAGRID High Performance Computing infrastructure. It is funded by ENEA, the Italian National Agency for New Technologies, Energy and Sustainable Economic Development and by Italian and European research programs, see http://www.cresco.enea.it/english for information

References

[1] F. Romanelli et al., Fusion electricity – a roadmap to the realization of fusion energy, European Fusion Development Agreement (EFDA) 2012, ISBN 978-3-00-040720-8

[2] G. Federici et al., Overview of EU DEMO design and R&D activities, Fusion Engineering and Design, 89 (2014), 882-889.

[3] C. Bachmann et al., Initial DEMO tokamak design configuration studies, Fusion Engineering and Design, 98-99 (2015), 1423-1426.

[4] P. Frosi, G. Mazzone, J. You, Structural design of DEMO Divertor Cassette Body: provisional FEM analysis and introductive application of RCC-MRx design rule, Fusion Engineering and Design, 109-111 (2016), 47-51

[5] P. Frosi, C. Bachmann et al., Structural analysis of DEMO Divertor Cassette Body and design study based on RCC-MRx, Fusion Engineering and Design, 124 (2017), 628-632.

[6] J. H. You, C. Bachmann, et al., Progress in the initial design activities for the European DEMO divertor: Subproject "Cassette". Fusion Engineering and Design, in press.
DOI: 10.1016/j.fusengdes.2017.03.018.

[7] EFDA_D_2MZ59L, G. Di Gironimo, Development of the CAD model of the Divertor system

[8] EFDA_D_2M5EEF, G. Di Gironimo, CAD Model of the Divertor CB system 2015

[9] ANSYS® Academic Research Mechanical, Release 18.2

[10] R.Villari et al., Neutron transport analysis through openings in in-vessel components, EFDA_D_2MEP2U

[11] P. A. Di Maio, S. Garitta, J. H. You, G. Mazzone, E. Vallone, M. Marino, Computational thermofluid-dynamic analysis of DEMO divertor cassette body cooling circuit, unpublished results. Paper presented to the 13th International Symposium on Fusion Nuclear Technology (ISFNT), September 25 - 29, 2017, Kyoto (Japan).

[12] P. A. Di Maio, S. Garitta, J. H. You, G. Mazzone, E. Vallone, Analysis of steady state thermal-hydraulic behaviour of the DEMO divertor cassette body cooling circuit, Fusion Engineering and Design, in press. DOI: 10.1016/j.fusengdes.2017.02.012.

[13] EFDA_D_2NAZYR, M. Roccella, EM DGM including TFCs and EM analyses of Plasma disruptions plus TFCs FD

[14] RCC-MRx 2012 AFCEN Edition, Design and Construction Rules for Mechanical Components of Nuclear Installation